Dalton Transactions

Accepted Manuscript

ROYAL SOCIETY OF CHEMISTRY

www.rsc.org/dalton

Journal Name

RSCPublishing

ARTICLE

Assemblies Of Salen-Type Oxidovanadium(IV) Complexes: Substituent Effects And In Vitro Proteintyrosine Phosphatase Inhibition

Cite this: DOI: 10.1039/xoxxoooooox

Received ooth January 2012,
Accepted ooth January 2012

DOI: 10.1039/xoxxoooooox

www.rsc.org/

Piotr Zabierowski*[a], Janusz Szklarzewicz[a], Ryszard Gryboś[a], Barbara Modryl[b] and Wojciech Nitek[a]

Oxidovanadium(IV) complexes with substituted chiral tetradentate dianionic *N,N*'-bis-*o*-hydroxybenzylidene-1,2-propylenediamines were synthesized and their physicochemical properties were characterized using single crystal X-ray diffraction, elemental analysis, ATR FTIR, UV-VIS and EPR spectroscopy, cyclic voltammetry, spectroelectrochemistry and preliminary *in vitro* protein-tyrosine phosphatase inhibition activity studies. Different 5-substituents in the salicylaldehyde (condensed with 1,2-diaminopropane; 2:1) were tested, namely 5-Br (complex 1), 5-Cl (2), 5-NO_2 (3) and 5-OCH_3 (4). The crystal structures of 1 and 2 show square pyramidal coordination of vanadium and parallel arrangement of monomeric *exo* isomers in supramolecular dimers. The halogen-halogen interaction of substituents in 5,5'-positions, leads to weakening of axial interaction between phenolate O and V in 2, compared to 1. Br atom takes part in halogen bonding with vanadyl group in 1. Complex 3 has a linear polymeric structure with V-O-V asymmetric bridge motif (IR absorption band at 873 cm^{-1}, separated *d-d* bands and broad EPR band structure in frozen solution pointing to oligomeric nature) while 4 is monomeric (V=O stretching at 976 cm^{-1}, broad *d-d* band structure). Redox potentials of the V^{4+}/V^{5+} couple lay in a range of -0.14-0.21 V (*vs*. Fc/Fc^{+}) and show substantial dependence on electron withdrawing properties of the substituents. The charge transfer character of the bands present in the range 365-395 nm was confirmed based on UV-VIS spectroelectrochemical experiments. Different assemblies of complex molecules are influenced by electron withdrawing properties of the 5,5'-substituents, leading to supramolecular dimers (1, 2 and 4) and linear polymeric self-assembly (3). *In vitro* study on representative 1, showed proteintyrosine phosphatase activity inhibition higher than suramin but lower than oxidovanadium(IV) sulphate and bis(maltolato)oxidovanadium(IV).

Introduction

N,N'-bis-*o*-hydroxybenzylideneethylenediamine, known as *salen*, is tetradentate dianionic ligand frequently incorporated in synthesis of coordination compounds with large number of metal cations. These metal complexes find applications *e.g.* in catalysis and molecular sensing.[1–15] Vanadium is very important transition metal in biological systems due to its ability to exist at different oxidation states and its affinity to oxygen.[16] Salen type oxidovanadium complexes were found to exhibit insulin-mimetic and protein-tyrosine phosphatase (PTP) inhibiting behavior.[17–22]

Interestingly, oxidovanadium(IV) *salen*-type complexes were found to exist in either monomeric or polymeric forms in solid state.[23,24] Oxidovanadium(IV) species with structures consisted of infinite polymeric chains bonded through V-O-V bridges are orange, brown or even black while the monomeric square pyramidal oxidovanadium(IV) species are usually green.[23] Quantum chemical calculations indicate that in these polymeric structures ferromagnetic interactions are favored between V^{IV} centers.[25] Donor properties of the vanadyl groups, studied extensively on Lewis adducts with compounds of 14 and 15 group elements, were shown to be dependent on steric factors of the ligand and *trans* coordination to oxido ligand.[26,27] Different homologues of [VO(salen)] have been synthesized, giving no straightforward evidence what is the key factor influencing these polymeric or monomeric assemblies.[28] The homologues consisted of aromatic and aliphatic β- and γ-diamines.[23,29–31] Even the flat systems comprised of aromatic diamine as a bridge between deprotonated *o*-hydroxy-benzylidene groups can be distorted from planarity in umbrella-

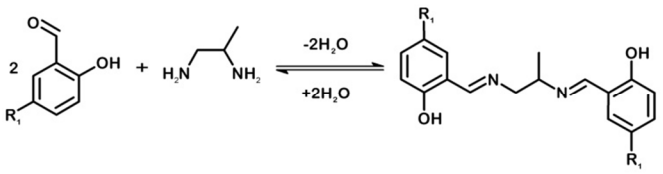

Scheme 1. Synthesis of *H_2dbsalpren* (R_1=Br), *H_2dcsalpren* (R_1=Cl), *H_2dnsalpren* (R_1=NO_2) and *H_2dmsalpren* (R_1=OMe) ligands.

like shape to afford polymeric structures.[23,29] Taking into consideration the previous findings we have decided to synthesize a series of oxidovanadium(IV) *N,N'*-bis-*o*-hydroxy-benzylidene-1,2-propylenediamine (*salpren*) complexes (see scheme 1), with different 5-substituents in the aromatic rings (salicylaldehyde) and methyl group (1,2-diaminopropane) running parallel to vanadyl bond, to see how do the electron withdrawing effects in combination with steric effects influence the crystal packing, nuclearity, solution behavior, redox and selected biological properties of the resulting compounds. To our knowledge, only few reports include X-ray crystal structures of oxidovanadium(IV) and oxidovanadium(V) complexes with chiral *salpren*, but none of them report systematic study on effects of 5,5'-substituents. In 1999 Leigh *et al.* reported X-ray crystal structure of 3,3'-dimethoxy substituted *salpren* oxidovanadium complex which is monomeric.[28] They have also reported structure of dimeric mixed valence V(IV)-V(V) complex with *salpren* and synthesis of 5,5'-dibromo substituted derivative in monomeric and polymeric form, but without crystal structures of them. Finally, in 2008 Chaudhury *et al*. reported X-ray crystal structure of dimeric *salpren* V(V)-V(V) diamagnetic oxido-species linked by OH bridge.[31]

Herein we present synthesis and characterization, including X-ray crystal structures, of a series of 5,5'-dibromo ([VO(dbsalpren)]; (1)], 5,5'-dichloro ([VO(dcsalpren)]; (2)], 5,5'-dinitro ({[VO(dnsalpren)]·H_2O}$_n$; (3)] and 5,5'-dimethoxy ([VO(dmsalpren)]; (4)] substituted *salpren* oxidovanadium(IV) complexes, discussion of their physicochemical properties and PTPs inhibition activity for representative complex 1.

Experimental Section

Materials and methods

All chemicals utilized in this work, excluding ethanol, were purchased from Sigma Aldrich at reagent grade purity and used without further purification. Ethanol for synthesis (92%) was purchased from Polmos (Poland). Microanalyses on carbon, hydrogen and nitrogen were performed using a VARIO MICRO CUBE elemental analyzer. Solvents used for electrochemical experiments were not additionally dehydrated. The UV-VIS spectra were recorded on SHIMADZU UV-VIS-NIR UV-3600 spectrophotometer with thermoelectrically temperature controlled CPS-240A CELL POSITIONER. The IR spectra were recorded on NICOLET IS5 FT-IR SPECTROMETER equipped with diamond crystal. Cyclic voltammetry measurements were carried out in dimethyl sulfoxide (DMSO) with $[Bu_4N]PF_6$ (tetrabuthyloammonium hexafluorophospate) (0.10 M) as the supporting electrolyte, using Pt disk as a working, Pt plate as a counter and silver chloride as a reference electrode on an AUTOLAB/PGSTAT 128N POTENTIOSTAT/GALVANOSTAT. Half-wave potential values, $E_{1/2}$, were calculated from the average anodic and cathodic peak potentials, $E_{1/2}=0.5(E_a+E_c)$. The redox potentials were calibrated versus ferrocene/ferrocenium (Fc^+/Fc) redox couple which was 0.44 V *vs*. silver chloride reference electrode under experimental conditions described herein. The magnetic susceptibility measurements were performed on SHERWOOD SCIENTIFIC magnetic susceptibility balance. Spectro-electrochemical cell was constructed from quartz cuvette (5 mm), platinum grid working electrode, silver wire pseudo-reference electrode and platinum plate counter electrode. Spectro-electrochemical measurements were carried out on coupled SHIMADZU UV-3600 and AUTOLAB/PGSTAT 128N Potentiostat/ Galvanostat. EPR spectra were recorded on BRUKER ELEXSYS 500 using 9.419 GHz microwave frequency. Simulations of EPR spectra were performed using EASYSPIN (functions `pepper` and `esfit`) toolbox for MATLAB.[32]

Diffraction data for single crystals of 1 and 2 were collected on the OXFORD DIFFRACTION SUPERNOVA four circle diffractometer, using the Mo (0.71069 Å) Kα radiation source and graphite monochromator. Cell refinement and data reduction was performed using firmware.[33] Positions of all of non-hydrogen atoms were determined by direct methods using SIR-97.[34] All non-hydrogen atoms were refined anisotropically using weighted full-matrix least-squares on $|F^2|$. Refinement and further calculations were carried out using SHELXL-97.[35] All hydrogen atoms joined to carbon atoms were positioned with an idealized geometry and refined using a riding model with U_{iso}(H) fixed at 1.5 U_{eq} of C for methyl groups and 1.2 U_{eq} of C for other. Graphics and geometrical calculations were carried out by using MERCURY.[36] CCDC-945963 (for 1), -945964 (for 2) include the supplementary crystallographic data for this work. These data can be obtained free of charge from The Cambridge Crystallographic Data Centre via www.ccdc.cam.ac.uk/data_request/cif.

Synthesis

[VO(dbsalpren)] (1)

50 mL of ethanolic solution of 5-bromosalicylaldehyde (201 mg; 1.00 mmol) and 1,2-diaminopropane (43 µl; 0.50 mmol) were refluxed for 45 minutes giving intensively yellow colored solution. To this solution $[VO(acac)_2]$ (133 mg; 0.500 mmol) was added and the color changed from yellow to dark green. After 40 minutes of refluxing the resulting precipitate was filtered off, washed with ethanol (30 mL) and dried in air. Yield 143 mg (56%). Anal. Calcd for $C_{17}H_{14}Br_2N_2O_3V$ (Mol. wt. 505.06 g/mol): C, 40.43; H, 3.18; N, 5.52 %. Found: C, 40.68; H, 3.54; N, 5.76 %. The single crystals suitable for X-ray diffraction were obtained after recrystallization in acetonitrile.

[VO(dcsalpren)] (2)

40 mL solution of 5-chlorosalicylaldehyde (157 mg; 1.00 mmol) and 1,2-diaminopropane (43 µl; 0.50 mmol) in 1-propanol was refluxed for 15 minutes, then $[VO(acac)_2]$ (133 mg; 0.500 mmol) was added and solution color changed from intensive yellow to dark green. The solution was refluxed for 30 minutes, then c.a. half of the initial volume of the solvent was evaporated at a rotary evaporator. The green crystalline precipitate was filtered off, washed with 10 mL of 1-propanol and dried in air. Yield: 138 mg (66%). Anal. Calcd for $C_{17}H_{14}Cl_2N_2O_3V$ (Mol. wt. 416.14 g/mol): C, 49.06; H, 3.39; N, 6.73 %. Found: C, 49.23; H, 3.40; N, 6.72 %. Crystals suitable for single crystal X-ray diffraction were obtained after recrystallization in acetonitrile.

$\{[VO(dnsalpren)]\ H_2O\}_n$ (3)

60 mL ethanolic suspension of 5-nitrosalicylaldehyde (346 mg; 2.00 mmol) was clarified by addition of triethylamine (278 µl; 2.00 mmol). After complete dissolution of the aldehyde, $[VO(acac)_2]$ (265 mg, 1.00 mmol) was added and the solution color changed to brown. This was refluxed until complete dissolution of $[VO(acac)_2]$, then 1,2-diaminopropane (86 µl, 1.00 mmol) was slowly added with instantaneous precipitation of an orange product. The suspension was refluxed for 30 minutes and then allowed to cool to the room temperature. The precipitate was filtered off, washed three times with acetone (30 mL) and dried in air. The synthesis without triethylamine also gives the same product, however larger amount of solvent is required due to low solubility of the aldehyde and resulting Schiff base. Yield: 400 mg (88.0%). Anal. Calcd for $C_{17}H_{16}N_4O_8V$ (Mol. wt. 455.27 g/mol): C, 44.85; H, 3.54; N, 12.31 %. Found: C, 45.43; H, 3.50; N, 12.32 %.

[VO(dmsalpren)] (4)

20 mL of ethanolic solution of 5-methoxysalicylaldehyde (124 µl, 1.00 mmol) was refluxed for 15 min with 1,2-diaminopropane (43 µl; 0.50 mmol) to form yellow solution. To this solution $[VO(acac)_2]$ (133 mg, 0.500 mmol) was added and refluxed for 30 minutes. The resulting dark green solution was concentrated to 10 mL, and allowed to cool at room temperature. The green crystalline precipitate was filtered off, washed with diethyl ether (20 mL) and dried in air. Yield: 105 mg (52%). Anal. Calcd for $C_{19}H_{20}N_2O_5V$ (Mol. wt. 407.31 g/mol): C, 56.03; H, 4.95; N, 6.88 %. Found: C, 55.90; H, 4.87; N, 6.84 %.

The magnetic susceptibility measurements at room temperature indicate on one unpaired electron for each of the compounds (1-4). The values of μ_{eff} are slightly lower than expected (0.1-0.3 units) for one unpaired electron. After grinding of 3, the magnetic moment increases from 1.4 to 1.7 of Bohr Magneton units.

In vitro biological evaluation of PTP1B, SHP1, SHP2 and LAR inhibition by an enzyme-based assay

PTPs are a large family of signaling enzymes that play an important role in signal transduction and regulation of cellular processes such as differentiation, cell growth and proliferation.[37–39] Deregulation of the PTPs activity can lead to aberrant signaling that can contribute to the development of various human diseases, such as diabetes and metabolic disorders.[40–43] Among various members in the PTPs superfamily, non-receptor, intracellular (PTP1B, SHP1 and SHP2) and receptor transmembrane-type PTPs (LAR - leukocyte common antigen-related protein tyrosine phosphatase) have been demonstrated to be a key negative regulator of insulin signaling through inactivating the insulin receptor by dephosphorylating tyrosine residues in the regulatory domain.[44,45] Several studies have provided evidence that vanadium compounds are strong inhibitors of tyrosine phosphatases.[46–50] Insulin-mimetic properties of many vanadium compounds have been reported in both *in vitro* and *in vivo* studies.[51–54] The main mode of their insulin-mimetic action is explained by inhibition of tyrosine phosphatases particularly PTP1B, LAR, SHP1 and SHP2 which are considered to be one of the best targets for diabetes and other metabolic disorders drug discovery.[41,43]

Test and reference compounds were dissolved in dimethyl sulfoxide (DMSO; its lack of PTP inhibiting activity has been experimentally excluded) at a concentration of 10 mM and further diluted in phosphate buffered saline (PBS). The final concentrations of compounds were 10 µM (14 mM concentration of DMSO) and 1 µM (1.4 mM concentration of DMSO). All reactions were carried out at room temperature in black, 384-well plates (Perkin Elmer). To the solution of the test compounds was added an equal volume of test solution phosphatase (PTP1B 50 ng/mL, SHP1 400 ng/mL, SHP2 50 ng/mL, LAR 5 ng/mL) in reaction buffer: 25 mM of 3-(*N*-morpholino) propanesulfonic acid (MOPS), 50 Mm NaCl, 1 mM dithiothreitol (DTT) and 0.05% Tween-20, pH 7.0. After 10 minutes, a solution of phosphate 6,8-difluoro-4-methyl (DiFMUP) was added until its final concentration was 0.1 mM. After 20 minutes incubation at room temperature, the fluorescence intensity (EX 355 EM 560 nm) was measured in a multifunction plate reader (POLARstar Omega, BMG Labtech, Germany).[55] Statistical analysis was performed by analysis of variance followed by the Tukey test for *post hoc* comparisons.

Results and Discussion

X-Ray crystal structures

The crystallographic parameters for 1 and 2 are given in table 1. The molecular structures of complexes 1 and 2 are depicted in fig. 1, together with atom labeling. The selected bond lengths are presented in table 2. Complexes 1 and 2 are monomeric *exo* isomers. The C10 atom in 1 and 2 is chiral and the crystals in both cases are racemic, containing equimolar amount of *R* and *S* enantiomers. In both cases vanadium(IV) is in square pyramidal geometry with oxido ligand coordinated axially and tetradentate Schiff base coordinated by the ONNO donor set. The distances of the V1 positions from ONNO mean planes of the square pyramid in 1 and 2 are close to 0.6 Å and these values are typical for VO^{2+} monomeric *salen* systems.[29,56]

Table 1. Crystallographic data for 1 and 2.

Complex	1	2
Empirical formula	$C_{17}H_{14}Br_2N_2O_3V$	$C_{17}H_{14}Cl_2N_2O_3V$
Formula weight	505.06	416.14
T	293(2) K	293(2) K
Crystal system	Monoclinic	Monoclinic
Space group	$P2_1/c$	$P2_1/c$
Unit cell dimensions	a = 13.5750(4) Å; α= 90° b = 9.8400(4) Å; β= 109.784(2)° c = 14.0040(5) Å; γ = 90°	a = 13.776(5) Å; α = 90° b = 9.987(5) Å; β = 113.198(5)° c = 13.703(5) Å; γ = 90°
Volume	1760.21(11) $Å^3$	1732.8(12) $Å^3$
Z	4	4
Density (calculated)	1.906 mg/m^3	1.595 mg/m^3
R[a]	0.0356	0.0517

a) $R=\Sigma(|F_o|- |F_c|)/\Sigma(|F_o|)$

Table 2. Selected bond lengths for 1 and 2 in [Å] (X= Cl or Br).

Valence Bond	1	2
V1-O22	1.588(3)	1.587(3)
C8-N9	1.282(4)	1.280(4)
N12-C13	1.273(4)	1.280(4)
O1-C2	1.317(4)	1.317(4)
C19-O20	1.320(4)	1.317(4)
C11-N12	1.488(4)	1.484(4)
N9-C10	1.486(4)	1.505(4)
V1-O22	1.588(3)	1.587(3)
X1-C5	1.907(3)	1.741(4)
X2-C16	1.899(3)	1.754(4)
V1-O1	1.924(2)	1.921(2)
V1-O20	1.946(2)	1.928(2)
V1-N9	2.072(3)	2.057(3)
V1-N12	2.066(3)	2.068(3)

The aliphatic tail C10-C21 (1.593(3) Å for 1 and 1.547(6) Å for 2) runs parallel to the V=O bond in both *exo* isomer molecules of 1 and 2 with O22-V1-C10-C21 dihedral angles of -11.2(3)º and -12.1(3)º for 1 and 2, respectively. The V=O bond lengths in complexes 1 and 2 are almost identical within experimental error and typical for double bond character in [VO(salen)] systems. The asymmetry introduced by the methyl group in diamine bridge manifests as slight differences in length between imine C=N bonds. Consequently, the C-N bond on the chiral carbon atom side is significantly elongated, especially in case of complex 2 (table 2), exhibiting unusually large value according to CSD database findings (Mogul). Small differences occur also in case of the carbon-halogen bonds. These bond lengths are equal in case of complex 1 while in 2 the difference between C-Cl bonds is rather significant (0.13 Å). The minor differences between molecular structures of 1 and 2 are associated with aromatic ring deviations from co-planarity with the basal plane of the square pyramid. This may be understood as an effect of intermolecular interactions in which the halogen atoms are involved. It was previously found that size and basicity of the halogen atom attached to the 5-position in salicylaldehyde part of the tridentate monoanionic compartmental Schiff base has a tremendous effect on formation of hydrogen bonds which can even lead to change of coordination geometry.[57,58]

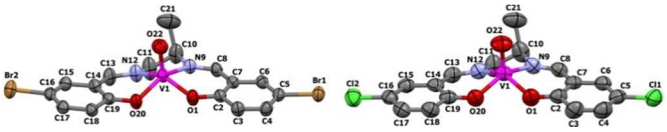

Figure 1. The molecular structures of complexes 1 (left side) and 2 (right side) together with atom labelling scheme. The hydrogen atoms were omitted for clarity. Thermal ellipsoids represent 50% of displacement probability.

However, in case of the tetradentate *salen*-type ligands described in this paper, the 5-bromo and 5-chloro substituents in salicylaldehyde half unit of the imine do not affect molecular assemblies in crystal lattices to such an extent. The crystal packing and hydrogen bonding of complexes 1 and 2 are presented in fig. 2. The hydrogen bond parameters are included in table 3. In both cases the supramolecular dimers, shown in fig. 2, are stacked by π-π interactions (with aromatic ring centroid-centroid distances of 3.79 and 4.06 Å for 1 and 2, respectively). The V···V distance in these dimers is 4.734(1) Å in 1 and 4.835(2) Å in 2, while the distance between V and phenolic oxygen of the neighboring molecule is 3.807(3) Å in 1 and 4.287(3) Å in 2. Such a substantial difference may be associated with slight disparity between basicity and size of Cl and Br atoms influencing parallel π-π stacking of the molecules in dimers due to halogen-halogen electrostatic repulsions. The crystal lattice of 1 contains only two types of hydrogen bonds (Table 3).[59] Therefore, the hydrogen bond network in 1 is consisted of one dimensional helical chains which may be described as $C^1_1(12)$, according to graph-set notation.[60] Beside hydrogen bonds, a halogen bond can be distinguished between vanadyl O22 oxygen and Br1' atom, with distance 3.242(2) Å.[61] In contrary, the Cl1 and Cl2 atoms in 2 take part in two intermolecular hydrogen bonds with aromatic ring sp^2 carbon atoms - C15' and C4', respectively. The vanadylic oxygen in 2 is hydrogen bonded to C18' aromatic carbon. Additionally, the phenolic O20 oxygen atom takes part in hydrogen bond with sp^3 C11'. All listed bonds give rise to total seven chain (for instance $C^1_1(12)$, $C^2_2(8)$,$C^2_2(24)$ and $C^1_2(6)$) and two ring motifs ($R^4_4(16)$ and $R^4_4(48)$), according to graph-set notation.

Table 3. Hydrogen bond parameters.

Complex	D---A	Distance [Å]	D-H···A	Angle [°]
1	C4'--- Br2	3.708(4)	C4'-H4'···Br2	135.3(3)
	C17'---Br1	3.773(4)	C17'-H17'···Br1	133.6(3)
2	C11---O20'	3.430(6)	C11-H11A···O20'	142.5(3)
	C15---Cl1'	3.586(4)	C15-H15···Cl1'	132.8(2)
	C4---Cl2'	3.727(4)	C4-H4···Cl2'	155.8(3)
	C18---O22'	3.514(5)	C18-H18···O22'	158.5(3)

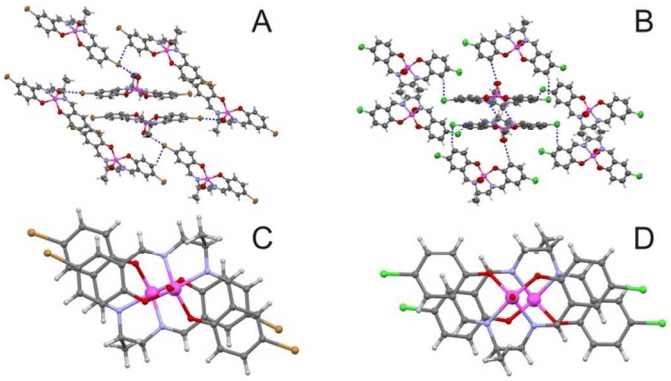

Figure 2. Intermolecular interactions (blue dashed line) in crystal structures of 1 (part A) and 2 (part B). View perpendicular to aromatic ring planes π-π stacked in supramolecular dimeric motif present in crystal structures of 1 (part C) and 2 (part D) in ball and stick representation. Thermal ellipsoids in part A and B are drawn with 50% of displacement probability and hydrogen atoms are shown as spheres of fixed radius.

Physicochemical characterization

UV-VIS SPECTROSCOPY

The spectra of the ligands *H_2dbsalpren* and *H_2dnsalpren* in DMSO are presented in figs. S1A and S1B (ESI) while the spectra of the complexes in DMSO and diffuse reflectance spectra are shown in fig. 3. The positions of the bands are presented in table 4. The ligands in DMSO solution exhibit very strong bands below 300 nm, which can be assigned to π→π* transitions.[62,63] Above 300 nm two bands occur which can be assigned to π→π* (*H_2dbsalpren*, 328 nm, logε=3,9) and n→π* (*H_2dbsalpren*, 406 nm, logε=2,4) transitions in the imine chromophore.[62] The *H_2dnsalpren* spectrum contains these two bands slightly red-shifted (λ_{max} 358 and 413 nm) in contrary to *H_2dbsalpren* and possesses additional bands ascribed to transitions in the NO_2 chromophore as shown in fig. S1B (band positions obtained after deconvolution of the spectrum 305, 324, 337, 358, 413 and 435 nm). In the spectra of the 1-4 complexes, bands associated with intra-ligand transitions are present within the range 240-280 nm (π→π*, n→π*).[63] The charge transfer transitions are positioned in the range 360-420 nm with values of molar absorption coefficients comparable to those for π→π* transitions in ligands but slightly red shifted.[64] With complex 4 this transition has the lowest energy in comparison to the rest of complexes (395 nm) what is associated with substituent effect of the methoxy group.

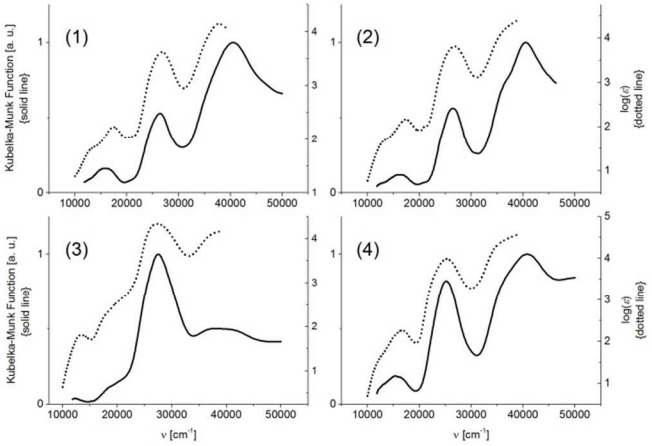

Figure 3. UV-VIS absorption spectra of 1-4 in DMSO at 295 K represented by dotted line (log(ε) as ordinate, right side scale) and UV-VIS diffuse reflectance spectra of the corresponding complexes at 295 K represented by solid line (Kubelka-Munk Function values as ordinate, left side scale).

Table 4. UV-VIS spectral data (diffuse reflectance – DR, absorption spectra in DMSO, sh-shoulder). In round brackets the log(ε) values are given for selected bands.

Complex; λ [nm] (logε)							
1		2		3		4	
DR	DMSO	DR	DMSO	DR	DMSO	DR	DMSO
248	---	245	---	246	257 (4.2)	240	---
---	264sh	275sh	273sh	264sh	---	280sh	285sh
386	373 (3.6)	376	373 (3.8)	370	367 (4.3)	376sh	395 (4.0)
---	410sh	---	402sh	407	---	416	437sh
580	575 (2.2)	582	576 (2.2)	506sh	566sh	599sh	592 (2.3)
659sh	660sh	671sh	657sh	---	---	669	664sh
801sh	744sh	808sh	728sh	813	745sh	757sh	766sh

Two transitions of *d-d* origin are present in the range 420-800 nm ($b_2 \rightarrow b_1$* and $b_2 \rightarrow e_\pi$*) while the third ($b_2 \rightarrow a_1$*), of the highest energy, is obscured by MLCT bands.[26] These two lower energy bands are overlapped in case of monomeric complexes 1, 2 and 4. In contrary, these bands are separated in spectrum of 3 – the $b_2 \rightarrow e_\pi$* transition is red shifted, while the $b_2 \rightarrow b_1$* transition is blue shifted in comparison to 1,2 and 4. This change, according to Cunningham *et al.*, is associated with different positions of vanadium nucleus in relation to the basal plane and elongation of the V=O bond.[26] Analysis of the spectra in DMSO solutions, especially the *d-d* bands, indicates that the broad band structure at *ca*. 600 nm may be associated with equilibrium between two types of species since the band structure is broad with distinguishable shoulder. The absorption spectrum of 3 indicates on larger separation of the *d-d* bands than in 1 and 2, similarly as in reflectance spectrum, what suggests presence of six coordinate form in solution.

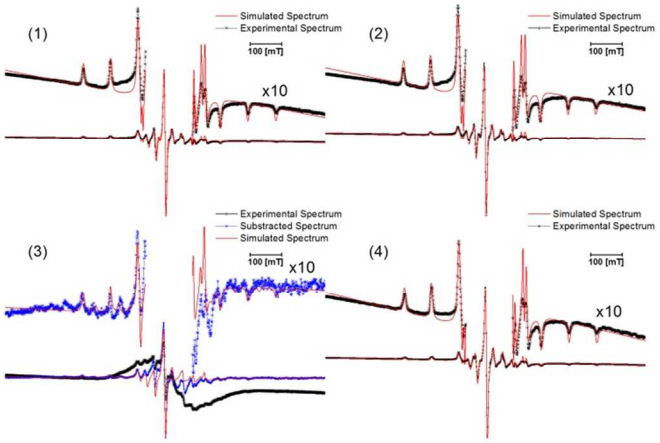

Figure 4. The EPR spectra of 1-4 in frozen (77 K) DMSO glass. Above wide field range spectra the magnified low field and high field fragments are presented. Each spectrum is accompanied by simulated spectrum for comparison.

EPR SPECTROSCOPY

The EPR spectra of the complexes 1-4 in DMSO glass at 77 K, together with simulated spectra are shown in fig. 4. The spin Hamiltonian parameters are included in table 5.

Table 5. Spin Hamiltonian parameters for 1-4 obtained from spectral simulations.

Complex/Spin system	$g_\perp$	$g_\parallel$	$A_\parallel$ [10^4 cm^{-1}]	$A_\perp$ [10^4 cm^{-1}]
1/S_1	1.971	1.951	156.5	52.5
1/S_2	1.973	1.952	156.9	47.7
2/S_1	1.974	1.953	156.5	52.5
2/S_2	1.978	1.957	156.9	47.7
3/S_1	1.977	1.955	157.0	51.9
3/S_2	1.980	1.964	133.8	50.9
4/S_1	1.972	1.951	156.5	52.4
4/S_2	1.972	1.953	156.9	47.5

Each of the spectrum is of axial nature with hyperfine structure indicating on interaction between one electron spin and ^{51}V nucleus. The simulations point to equilibrium between at least two spin systems for frozen solutions of 1-4. In case of 1, 2 and 4 the systems differ slightly in $A_\perp$ values what can be understood in terms of different equatorial coordination of *salpren* ligand in isomers existing in DMSO solution (possible *exo-endo* isomerism). The broad band structure observed for 3 may associated with interactions of V^{IV} centers in oligomeric chains. Analogous broad band structure is characteristic for similar interactions in V^{IV} based nanotubes.[65] The hyperfine coupling constant $A_\parallel$=133.8x10^4 cm^{-1} indicates on distorted octahedral coordination of V^{IV} center for one spin system in a mixture.[61] The second spin system in solution of 3 has almost identical spin Hamiltonian parameters as in case of 1, 2 and 4.

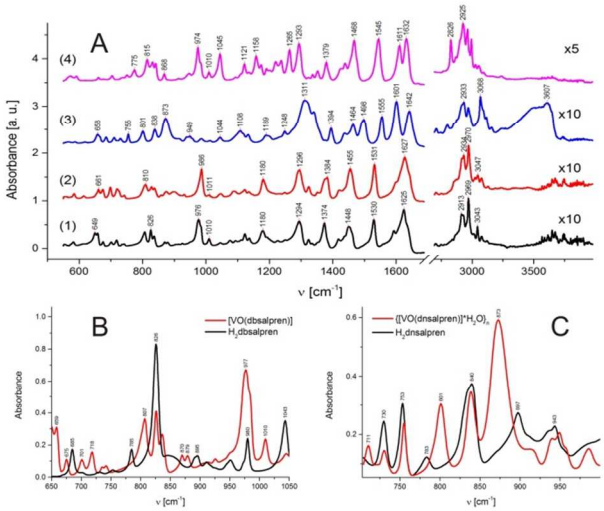

Figure 5. ATR FTIR spectra of complexes 1-4 (part A) with magnification of the range above 2750 cm^{-1} (scale of magnification given on the right side of part A);. Narrow range ATR FTIR spectra of isolated ligands *H_2dbsalpren* (part B) and *H_2dnsalpren* (part C) together with narrow range spectra of the corresponding complexes. Given numbers (in cm^{-1}) are positions of the selected bands. Room temperature.

This may be understood as a result of equilibrium between polymeric and monomeric species in solution.

IR SPECTROSCOPY

The IR spectra for complexes 1-4 are presented in fig. 5 together with band positions. The spectra of the ligands *H_2dbsalpren* and *H_2dnsalpren* in a range 600-1100 cm^{-1} are presented in fig. 5B and 5C together with spectra of the corresponding complexes. The bands in the range of 1600-1642 cm^{-1} are ascribed to a stretching vibration of the C=N bond and due to different chemical surroundings and occurrence of resonance, one or two distinct bands may be distinguished.[66,67] In the spectrum of 3, a broad band is observed at 1314 cm^{-1}, which is associated with an asymmetric bending vibration of the NO_2 group.[66] The spectrum of 4 consists of a very strong band at 1045 cm^{-1} which corresponds to C-O stretching vibration of the methoxy substituent.[66] A very weak and broad band with center at 3607 cm^{-1} may be distinguished only in case of 3, what is associated with presence of crystallization water molecules weakly H-bonded in the crystal lattice, as can be inferred from relatively high O-H stretching vibration energy.[68] This finding is consistent with elemental analysis results. Very important information can be extracted from analysis of spectra in the range 850-1000 cm^{-1} shown in figs. 5B and 5C. The ligands absorb very weakly in this range of wavenumbers. Very strong bands corresponding to the V=O stretching vibration are present in the spectra of 1, 2 and 4 in the 970-990 cm^{-1} range.[26,69] The frequencies of these bands are similar for 1 and 4 (974-976 cm^{-1}) and slightly shifted to higher energy in case of 2 (986 cm^{-1}). This shift may be associated with different parallel assembly of dimers in the solid state. According to Cunningham *et al.*, donation of electron density from vicinal phenolic oxygen to vanadium center (in supramolecular dimer)

results in shift of the V=O stretching band to higher energies.[26] Halogen bonding in 1 seems to have significant effect on energy of this stretching band (decrease), since its frequency should be higher than in 2, taking into consideration the significant phenolate group donation to vanadium center in 1. Similarly, in case of complex 4 the hydrogen bonding between oxygen of methoxy group and V=O group may be associated with relatively lower energy of this band in comparison to spectrum of complex 2. Interestingly, the band υ(V=O) is not present in spectrum of 3. Instead, a band at 873 cm^{-1} can be distinguished (fig. 5C). The ligand does not absorb in this region what clearly indicates on a stretching V-O vibration (weakening of V=O bond order) in the asymmetric V-O-V bridge, characteristic for polymeric [VO(salen)] type structures.[69]

Cyclic Voltammetry

The cyclic voltammograms of the complexes in DMSO are presented in fig. 6A. Each compound exhibit quasi reversible redox couple with $E_{1/2}$ in the range -0.14-0.21 V and irreversible cathodic wave at ca. -2.0 V. The half wave potentials for complexes 1-4 are presented in table 6. The high potential quasi-reversible couple, with redox potentials dependent on substituent, is ascribed to V(V)/V(IV) redox couple.[12,64,70] The reported redox potentials strongly correlate with Hammet substituent constants, as shown in table 6.[71] The redox potentials of 1 and 2 are close to the literature value reported for $[VO(salen)]^{0/+}$ redox couple.[12,70,72,73] Complex 3, with the highest $E_{1/2}$ redox potential in described family of complexes, requires larger driving force to be oxidized and as a result the fourth oxidation state of vanadium is better stabilized than in case of the rest complexes.

The irreversible peak at *ca*. -2.0 V (for 1, 2 and 4) and -1.8 V (for 3), assigned to reduction to V(III), can be reversed only in case of 3 when the timescale of the electrochemical experiment is sufficiently shortened using higher sweep rates (at 1 V/s sweep rate the couple is almost reversible).[74] This indicates that after reduction to V(III) the V=O bond breakage occurs and this process is slowest in case of 3, while the higher cathodic potential for 3 (-1.8 V) suggests that V^{4+} centre is easier to reduce in comparison to the rest of the complexes.[74] Complexes 1, 2 and 4 exhibit only irreversible redox processes in this range of potentials and the same potential sweep rates. This indicates that Lewis acidity of the vanadium center can be modulated by the *p*-position to phenolic group in *salpren* oxidovanadium complexes. Such tuning of properties may be successfully applied in design of sensor electrode materials for obtaining lower detection limits and higher stabilization of V(IV) to oxidation by atmospheric oxygen.[12]

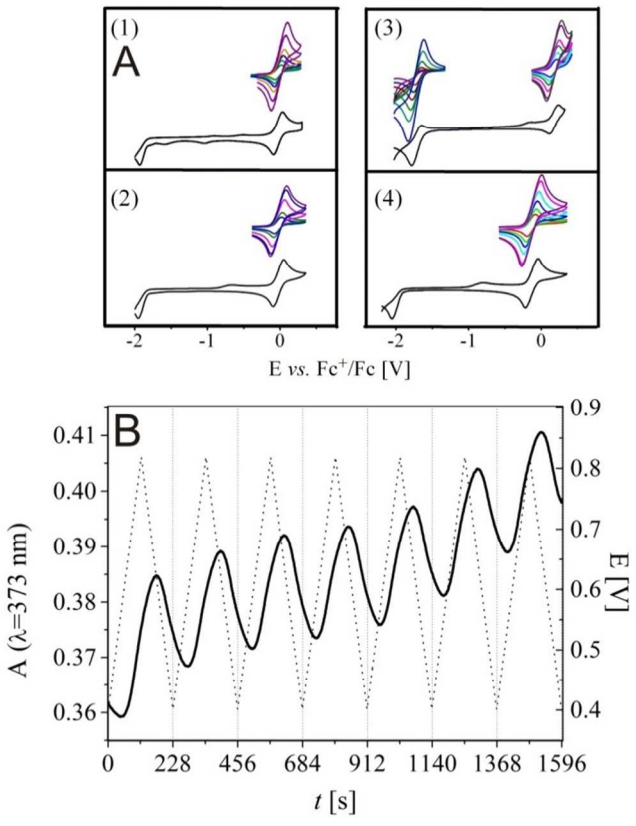

Figure 6. Cyclic voltammograms of complexes 1-4 in DMSO solution at 295 K (part A). The wide range (black line) current-potential curves were registered with 100 mV/s sweep rate while the upper narrow range curves were registered with different values of potential sweep rate: 20, 50, 100, 200, 500 and 1000 mV/s (with increasing peak current). Spectroelectrochemistry of representative complex 2 in DMSO at room temperature (part B). The values of absorbance at 373 nm (left side ordinate) in time (abscissa), represented by black solid line accompanied by potential-time (right side ordinate) curve represented as black dotted line.

Table 6. Redox potentials for 1-4 in DMSO. Room temperature. (σ_p denotes Hammet constant for *para* substituent to phenolic group).[71]

Complex	$E_{1/2}$ [V]	ΔE [V]	σ_p
1	-0.070	0.115	0.23
2	-0.019	0.147	0.23
3	0.208	0.143	0.78
4	-0.135	0.135	-0.27

Spectroelectrochemistry

In fig. 6B the potential and absorbance transients in time are presented for representative complex 2. The absorbance at 373 nm is decreasing during oxidation and increasing during reduction. A delay between redox process and absorbance change is governed by diffusion of absorbing redox species. Such behavior is in agreement with assumption that the quasi-reversible peak is associated with redox couple V^{4+}/V^{5+}. Similar curves have been detected for complexes 3 and 4. The absorbance at 373 nm for 1 is slightly decreasing during subsequent redox cycles in DMSO and under elevated temperature in time (fig. S1) but at room temperature complex is stable. The absorbance-time transients of the same type were collected at 572 nm indicating metal centered processes (*d-d* bands are disappearing on oxidation to V^{5+}) and charge transfer origin of the transitions at 373 nm.

Inhibition Of PTP1B, SHP1, SHP2 And LAR By An Enzyme-Based Assay

The effect of complex 1, $[VO(mal)_2]$, $VOSO_4$ and suramin (which known as a potent, reversible and competitive inhibitor of PTP1B)[75] on PTPs activity in *in vitro* screening assay is given in table 7. The results are expressed as percent of intensity of emission at 560 nm related to control without added compound. The observed order of non-receptor intracellular PTPs inhibition PTP1B < SHP2 < SHP1 is the same for all vanadium compounds at 10 μM concentration. Suramin exhibits the strongest inhibition of PTP1B, SHP1 and LAR. However, the degree of PTP inhibition activity of suramin in comparison to the studied vanadium compounds is substantially lower.

Comparison of PTPs inhibition activity of 1 and reference vanadium compounds needs to be considered with awareness of several factors significantly affecting the observed biological response. These factors have been widely investigated by Crans *et al*. who reported for the first time PTPs inhibition by coordination complexes of vanadium.[49,50] One of these factors, is speciation of $VOSO_4$ under experimental conditions.[76,77] Aqueous 10^{-6}-10^{-5} molar solutions of $VOSO_4$ at neutral pH contain predominantly an EPR silent dimeric form $[(VO)_2(OH)_5]^-$ while in aerobic conditions large part of V(IV) is oxidized to V(V).[77] As a result, equilibrium is reached in the system, whereby concentration of monomeric vanadyl cation is low and alters non-linearly with diluted amount of $VOSO_4$.[76,77] This equilibrium is perturbed when an organic ligand is complexed by vanadium.[49] In many situations either vandium species may bind to certain components of the assay i.e. buffers, or PTPs are sensitive to components of the assay and therefore biological response may be profoundly affected.[49,78] Nevertheless, depending on thermodynamic stability of these complexes and ability to maintain certain oxidation state of vanadium under aerobic atmosphere, the concentration of vanadyl cation is usually low under experimental conditions.[76,77] However, as crystallographically evidenced by Peters *et al*. in study on $[VO(mal)_2]$, it is not vanadyl but unligated vanadate anion (VO_4^{3-}) which binds to PTPs domains and thus exhibits PTPs inhibiting behavior in a manner of a transition state analogue.[79] This may suggest that organovanadium compounds are only source of vanadium not directly interacting with PTPs domains. However, study reported by Guo *et al*. on stable biguanido oxovanadium(IV) complexes with metformin, phenformin and moroxydine showed excellent potency of these complexes as PTPs inhibitors (IC_{50} values of nM order of magnitude) and substantial dependence of biological response on a type of phospatase and the chemical nature of the organic ligand (bulkiness and hydrogen bond participation) in oxidovandium(IV) complex.[80] This might suggest that when an organovanadium complex approach a PTP domain it is partly bound in a pocket of an enzyme whereby the organic ligand is subsequently exchanged on water molecules and V(IV) is oxidized to V(V), forming vanadate anion. Consequently, the successful organic ligand should not be too strongly bound to vanadium center and thus tetradentate ONNO donating ligands, such as *salen*, are rather poor candidates in an *in vitro* study, since trigonal bypiramidal geometry is supported in PTPs domain.[81] Indeed, such behavior of [VO(salpren)] type compound (1) confirms this anticipation. The results presented in table 7 indicate on a weaker (*ca*. 3-6 times) with PTP1B, SHP1, SHP2 and a much weaker (*ca*. 5-11 times) with LAR inhibiting activity of 1 than $VOSO_4$ and $[VO(mal)_2]$ at 10 μM concentration of vanadium. At 1 μM concentration, the inhibiting activity of 1 is comparable to $VOSO_4$ with each studied PTPs and almost twice weaker than $[VO(mal)_2]$ with PTP1B, slightly weaker with LAR and comparable with SHP1 and SHP2. Similar inhibition of 1 at 1 μM and $VOSO_4$ suggests that the speciation of 1 in conditions of the assay may lead to formation of either low amounts of vanadate after oxidation of V(IV) and hydrolysis of the *salpren* Schiff base, or dimeric species with ONN donating *salpren*-type ligand (partial *salpren* hydrolysis) reported by Xie *et al*.[21] Interestingly, under current conditions of the assay, inhibiting potency of $[VO(mal)_2]$ against PTP1B is almost twice larger than $VOSO_4$ at applied concentrations of vanadium. These results are not in agreement with the order of previously reported K_i values for $VOSO_4$ and $[VO(mal)_2]$, which are slightly lower for $VOSO_4$, albeit this divergence is 0.5 μM.[79,82] Such differences in obtained results may be a consequence of disparity in assay conditions i.e. incubation time and buffers composition.[82] Another important factor influencing observed biological response may be a temperature of incubation. In conclusion, presented results unambiguously indicate on poorer *in vitro* PTPs inhibition of [VO(salpren)] type compounds than $VOSO_4$ and $[VO(mal)_2]$ but higher than suramin. Nonetheless, this preliminary *in vitro* study does not exclude an *in vivo* antidiabetic activity of 1, since dimeric $[V_2O_2(\mu\text{-}O)_2(L)_2]$ (where L is tridentate ONN salen type ligand) and water soluble $[VO(salen\text{-}SO_3)]^{2-}$ compounds exhibit such promising behavior.[21,22]

Table 7. The results of *in vitro* PTPs inhibition activity study of selected vanadium complexes and suramin.

PTPas activity (% of control, mean ± SD)				
Concentration of compound 10 μM				
Compound	PTP1B	SHP1	SHP2	LAR
(1)	56±2	28±1	17±1	39±3
$[VO(mal)_2]$	10±1	9.1±0.1	4.7±0.1	3.6±0.1
$VOSO_4$	21±1	8.0±0.3	4.9±0.1	7.7±0.1
suramin	81±1	69±1	110±10	100±10
Concentration of compound 1 μM				
Compound	PTP1B	SHP1	SHP2	LAR
(1)	42±2	25±2	20±1	63±2
$[VO(mal)_2]$	23±1	24±1	18±1	42±1
$VOSO_4$	38±1	30±1	23±1	56±1
suramin	93±2	83±2	100±10	91±2

Conclusions

We have shown that the electron withdrawing properties of substituents in *para* position to phenolic group of *salpren* oxidovanadium(IV) complexes influence acidity of the vanadium center, what leads to different assemblies and physicochemical properties. Strongly electron withdrawing substituents lead to polymeric linear V-O-V structures, what can be qualitatively understood as an increase of Lewis acidity of the vanadium center. The discussed differences in physicochemical properties for polymeric and monomeric species are significant, including redox potentials, solubility and spectroscopic features. This fine tuning of acidity of vanadium center by substituents may find application in designing of novel molecular sensors with lower analyte detection limits. The *in vitro* PTPs inhibition studies on 1, revealed that the complex exhibits lower activity than $VOSO_4$ and $[VO(mal)_2]$ but higher than suramin.

Aknowledgements

This work was partly financed by European Regional Development Found under the Innovative Economy Programme 2007-2013 (WND POIG.01.03.01-174/09).

Notes and references

[a]Faculty of Chemistry, Jagiellonian University, Ingardena 3, 30-060 Kraków, Poland
[b]Faculty of Pharmacy, Jagiellonian University Medical College, Medyczna 9, Kraków 30-688, Poland
Electronic Supplementary Information (ESI) available: UV-VIS spectral data concerning thermal stability and stability of 1 under natural pH. See DOI: 10.1039/b000000x/

1. P. G. Cozzi, *Chem. Soc. Rev.*, 2004, **33**, 410–421.
2. D. J. Darensbourg, *Chem. Rev.*, 2007, **107**, 2388–2410.
3. T. Katsuki, *Coord. Chem. Rev.*, 1995, **140**, 189–214.
4. T. Katsuki, *Chem. Soc. Rev.*, 2004, **33**, 437–444.
5. H. Komatsu, B. Ochiai, and T. Endo, *J. Polym. Sci. Part Polym. Chem.*, 2008, **46**, 3673–3681.
6. C. S. Martin, T. R. L. Dadamos, and M. F. S. Teixeira, *Sens. Actuators B Chem.*, 2012, **175**, 111–117.
7. M. R. Maurya, A. Kumar, P. Manikandan, and S. Chand, *Appl. Catal. Gen.*, 2004, **277**, 45–53.
8. A. Pui and J.-P. Mahy, *Polyhedron*, 2007, **26**, 3143–3152.
9. E. Tsuchida, K. Oyaizu, E. L. Dewi, T. Imai, and F. C. Anson, *Inorg. Chem.*, 1999, **38**, 3704–3708.
10. E. Tsuchida and K. Oyaizu, *Coord. Chem. Rev.*, 2003, **237**, 213–228.
11. K. Yamamoto, K. Oyaizu, and E. Tsuchida, *J. Am. Chem. Soc.*, 1996, **118**, 12665–12672.
12. H. Kanso, N. Inguimbert, L. Barthelmebs, G. Istamboulie, F. Thomas, C. Calas-Blanchard, and T. Noguer, *Chem. Commun.*, 2014, **50**, 1658-1661.
13. A. Zulauf, M. Mellah, X. Hong, and E. Schulz, *Dalton Trans.*, 2010, **39**, 6911–6935.
14. P. A. Raymundo-Pereira, M. F. S. Teixeira, O. Fatibello-Filho, E. R. Dockal, V. G. Bonifácio, and L. H. Marcolino-Junior, *Mater. Sci. Eng. C*, 2013, **33**, 4081–4085.
15. S. Barman, S. Patil, J. Desper, C. M. Aikens, and C. J. Levy, *Eur. J. Inorg. Chem.*, 2013, **2013**, 5708–5717.
16. Z. Liu and F. C. Anson, *Inorg. Chem.*, 2000, **39**, 274–280.
17. I. Correia, J. C. Pessoa, M. T. Duarte, R. T. Henriques, M. F. M. Piedade, L. F. Veiros, T. Jakusch, T. Kiss, Á. Dörnyei, M. M. C. A. Castro, C. F. G. C. Geraldes, and F. Avecilla, *Chem. - Eur. J.*, 2004, **10**, 2301–2317.
18. N. Durai and G. Saminathan, *J. Clin. Biochem. Nutr.*, 1997, **22**, 31–39.
19. J. M. Lacoste, J. Duhault, and D. Ravel, *EUR Pat Appl EP*, 1993, **521**, 787.
20. S. Roy, A. K. Mondru, S. K. Dontamalla, R. P. Vaddepalli, S. Sannigrahi, and P. R. Veerareddy, *Biol. Trace Elem. Res.*, 2011, **144**, 1095–1111.
21. M. Xie, X.-D. Yang, W. Liu, S. Yan, and Z. Meng, *J. Inorg. Biochem.*, 2010, **104**, 851–857.
22. M. Li, D. Wei, W. Ding, B. Baruah, and D. C. Crans, *Biol. Trace Elem. Res.*, 2008, **121**, 226–232.
23. M. Kojima, H. Taguchi, M. Tsuchimoto, and K. Nakajima, *Coord. Chem. Rev.*, 2003, **237**, 183–196.
24. K. Fujiwara and T. Ishida, *Polyhedron*, 2011, **30**, 3073–3078.
25. N. Matsuoka, M. Tsuchimoto, and N. Yoshioka, *J. Phys. Chem. B*, 2011, **115**, 8465–8473.
26. B. Cashin, D. Cunningham, P. Daly, P. McArdle, M. Munroe, and N. Ní Chonchubhair, *Inorg. Chem.*, 2002, **41**, 773–782.
27. N. F. Choudhary, P. B. Hitchcock, G. J. Leigh, and S. W. Ng, *Inorganica Chim. Acta*, 1999, **293**, 147–154.
28. N. F. Choudhary, N. G. Connelly, P. B. Hitchcock, and G. J. Leigh, *J. Chem. Soc. Dalton Trans.*, 1999, 4437–4446.
29. K. Nakajima, M. Kojima, S. Azuma, R. Kasahara, M. Tsuchimoto, Y. Kubzono, H. Maeda, S. Kashino, S. Ohba, Y. Yoshikawa, and J. Fujita, *Bull. Chem. Soc. Jpn.*, 1996, **69**, 3207–3216.
30. P. Adão, J. Costa Pessoa, R. T. Henriques, M. L. Kuznetsov, F. Avecilla, M. R. Maurya, U. Kumar, and I. Correia, *Inorg. Chem.*, 2009, **48**, 3542–3561.
31. P. B. Chatterjee, D. Mandal, A. Audhya, K.-Y. Choi, A. Endo, and M. Chaudhury, *Inorg. Chem.*, 2008, **47**, 3709–3718.
32. S. Stoll and A. Schweiger, *J. Magn. Reson.*, 2006, **178**, 42–55.
33. *CrysAlis PRO*, Agilent Technologies, Oxford, United Kingdom, 2010.
34. A. Altomare, M. C. Burla, M. Camalli, G. L. Cascarano, C. Giacovazzo, A. Guagliardi, A. G. G. Moliterni, G. Polidori, and R. Spagna, *J. Appl. Crystallogr.*, 1999, **32**, 115–119.
35. G. M. Sheldrick, *SHELXL-97*, 1997.
36. C. F. Macrae, I. J. Bruno, J. A. Chisholm, P. R. Edgington, P. McCabe, E. Pidcock, L. Rodriguez-Monge, R. Taylor, J. van de Streek, and P. A. Wood, *J. Appl. Crystallogr.*, 2008, **41**, 466–470.
37. A. Cheng, N. Dubé, F. Gu, and M. L. Tremblay, *Eur. J. Biochem.*, 2002, **269**, 1050–1059.
38. A. W. Stoker, *J. Endocrinol.*, 2005, **185**, 19–33.
39. W. J. A. J. Hendriks, A. Elson, S. Harroch, and A. W. Stoker, *FEBS J.*, 2008, **275**, 816–830.
40. K. Yamauchi, K. L. Milarski, A. R. Saltiel, and J. E. Pessin, *Proc. Natl. Acad. Sci.*, 1995, **92**, 664–668.
41. J. M. Zabolotny, Y.-B. Kim, O. D. Peroni, J. K. Kim, M. A. Pani, O. Boss, L. D. Klaman, S. Kamatkar, G. I. Shulman, B. B. Kahn, and B. G. Neel, *Proc. Natl. Acad. Sci.*, 2001, **98**, 5187–5192.
42. K. Hayashi, K. Shibata, T. Morita, K. Iwasaki, M. Watanabe, and K. Sobue, *J. Biol. Chem.*, 2004, **279**, 40807–40818.
43. S. Koren and I. G. Fantus, *Best Pract. Res. Clin. Endocrinol. Metab.*, 2007, **21**, 621–640.
44. A. Alonso, J. Sasin, N. Bottini, I. Friedberg, I. Friedberg, A. Osterman, A. Godzik, T. Hunter, J. Dixon, and T. Mustelin, *Cell*, 2004, **117**, 699–711.
45. L. Bialy and H. Waldmann, *Angew. Chem. Int. Ed.*, 2005, **44**, 3814–3839.
46. K. G. Peters, M. G. Davis, B. W. Howard, M. Pokross, V. Rastogi, C. Diven, K. D. Greis, E. Eby-Wilkens, M. Maier, A. Evdokimov, S. Soper, and F. Genbauffe, *J. Inorg. Biochem.*, 2003, **96**, 321–330.
47. C. C. McLauchlan, J. D. Hooker, M. A. Jones, Z. Dymon, E. A. Backhus, B. A. Greiner, N. A. Dorner, M. A. Youkhana, and L. M. Manus, *J. Inorg. Biochem.*, 2010, **104**, 274–281.
48. R. Gryboś, P. Paciorek, J. T. Szklarzewicz, D. Matoga, P. Zabierowski, and G. Kazek, *Polyhedron*, 2013, **49**, 100–104.
49. D. C. Crans, R. L. Bunch, and L. A. Theisen, *J. Am. Chem. Soc.*, 1989, **111**, 7597–7607.
50. D. C. Crans, A. D. Keramidas, and C. Drouza, *Phosphorus Sulfur Silicon Relat. Elem.*, 1996, **109**, 245–248.
51. M. Krosniak, Z. Zachwieja, B. Filipek, M. Zygmunt, and R. Grybos, *Arch. Pharm. (Weinheim)*, 2001, **334**, 388–392.

52. S.-Q. Zhang, X.-Y. Zhong, W.-L. Lu, L. Zheng, X. Zhang, F. Sun, G.-Y. Fu, and Q. Zhang, *J. Inorg. Biochem.*, 2005, **99**, 1064–1075.
53. A. Sheela, S. M. Roopan, and R. Vijayaraghavan, *Eur. J. Med. Chem.*, 2008, **43**, 2206–2210.
54. T. Kiss, T. Jakusch, D. Hollender, A. Dörnyei, E. A. Enyedy, J. C. Pessoa, H. Sakurai, and A. Sanz-Medel, *Coord. Chem. Rev.*, 2008, **252**, 1153–1162.
55. S. Welte, K.-H. Baringhaus, W. Schmider, G. Müller, S. Petry, and N. Tennagels, *Anal. Biochem.*, 2005, **338**, 32–38.
56. G. Hoshina, M. Tsuchimoto, and S. Ohba, *Acta Crystallogr. C*, 1999, **55**, 1812–1813.
57. P. Zabierowski, J. Szklarzewicz, K. Kurpiewska, K. Lewiński, and W. Nitek, *Polyhedron*, 2013, **49**, 74–83.
58. P. Zabierowski, J. Szklarzewicz, and W. Nitek, *Acta Crystallogr. C*, 2014, **70**, 659–661.
59. A. Kovacs and Z. Varga, *Coord. Chem. Rev.*, 2006, **250**, 710–727.
60. M. C. Etter, *Acc. Chem. Res.*, 1990, **23**, 120–126.
61. M. Domagała, P. Matczak, and M. Palusiak, *Comput. Theor. Chem.*, 2012, **998**, 26–33.
62. P. Jeslin Kanaga Inba, B. Annaraj, S. Thalamuthu, and M. A. Neelakantan, *Spectrochim. Acta. A. Mol. Biomol. Spectrosc.*, 2013, **104**, 300–309.
63. A. C. Braithwaite, P. E. Wright, and T. N. Waters, *J. Inorg. Nucl. Chem.*, 1975, **37**, 1669–1674.
64. J. C. Dutton, G. D. Fallon, and K. S. Murray, *Inorg. Chem.*, 1988, **27**, 34–38.
65. C. J. Magon, J. F. Lima, J. P. Donoso, V. Lavayen, E. Benavente, D. Navas, and G. Gonzalez, *J. Magn. Reson.*, 2012, **222**, 26–33.
66. G. Socrates, *Infrared and Raman characteristic group frequencies: tables and charts*, Wiley, Chichester, 3rd ed., 2001.
67. P. Plitt, H. Pritzkow, T. Oeser, and R. Kraemer, *J. Inorg. Biochem.*, 2005, **99**, 1230–1237.
68. A. Kocak, G. Austein-Miller, W. L. Pearson, G. Altinay, and R. B. Metz, *J. Phys. Chem. A*, 2013, **117**, 1254–1264.
69. M. Mathew, A. J. Carty, and G. J. Palenik, *J. Am. Chem. Soc.*, 1970, **92**, 3197–3198.
70. Y. Sasajima, M. Shimizu, N. Kuroyanagi, N. Kishikawa, K. Noda, S. Itoh, H. D. Takagi, and M. Inamo, *Inorganica Chim. Acta*, 2006, **359**, 346–354.
71. C. Hansch, A. Leo, and R. W. Taft, *Chem. Rev.*, 1991, **91**, 165–195.
72. K. Oyaizu, N. Hayo, Y. Sasada, F. Kato, and H. Nishide, *Dalton Trans.*, 2013, **42**, 16090–16095.
73. P. Galloni, A. Coletti, B. Floris, and V. Conte, *Inorganica Chim. Acta*, 2014, **420**, 144–148.
74. A. Kapturkiewicz, *Inorganica Chim. Acta*, 1981, **53**, L77–L79.
75. D. F. McCain, L. Wu, P. Nickel, M. U. Kassack, A. Kreimeyer, A. Gagliardi, D. C. Collins, and Z.-Y. Zhang, *J. Biol. Chem.*, 2004, **279**, 14713–14725.
76. D. C. Crans, J. J. Smee, E. Gaidamauskas, and L. Yang, *Chem. Rev.*, 2004, **104**, 849–902.
77. D. C. Crans, K. A. Woll, K. Prusinskas, M. D. Johnson, and E. Norkus, *Inorg. Chem.*, 2013, **52**, 12262–12275.
78. M. Li, W. Ding, B. Baruah, D. C. Crans, and R. Wang, *J. Inorg. Biochem.*, 2008, **102**, 1846–1853.
79. K. G. Peters, M. G. Davis, B. W. Howard, M. Pokross, V. Rastogi, C. Diven, K. D. Greis, E. Eby-Wilkens, M. Maier, A. Evdokimov, S. Soper, and F. Genbauffe, *J. Inorg. Biochem.*, 2003, **96**, 321–330.
80. L. Lu, X. Gao, M. Zhu, S. Wang, Q. Wu, S. Xing, X. Fu, Z. Liu, and M. Guo, *BioMetals*, 2012, **25**, 599–610.
81. D. C. Crans, M. L. Tarlton, and C. C. McLauchlan, *Eur. J. Inorg. Chem.*, 2014, DOI: 10.1002/ejic.201402306.
82. A. P. Seale, L. A. de Jesus, S.-Y. Kim, Y.-H. Choi, H. B. Lim, C.-S. Hwang, and Y.-S. Kim, *Biotechnol. Lett.*, 2005, **27**, 221–225.

Table of Contents

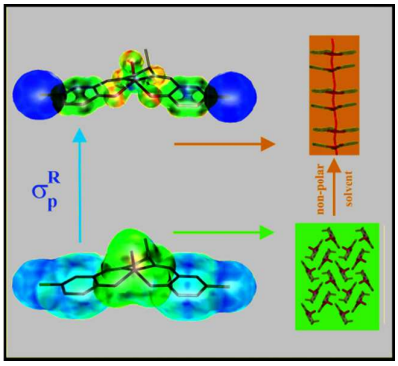

Systematic study on 5,5'-disubstituted oxidovanadium(IV) complexes with chiral salen type ligand showed variable assemblies of complex molecules dependent on steric and electronic factors of the substituents.